Dissociation of CH_3-O as a Driving Force for Methoxyacetophenone Adsorption on Si(001)

Kane M. O'Donnell,[†] Carly Byron,[‡] Gareth Moore,[¶] Lars Thomsen,[§]

Oliver Warschkow,[‖] Andrew Teplyakov,[‡] and Steven R. Schofield[*,¶,⊥]

[†]*Department of Physics and Astronomy, Curtin University, Bentley, Western Australia 6102, Australia.*

[‡]*Department of Chemistry and Biochemistry, University of Delaware, Newark, Delaware 19716, United States.*

[¶]*Department of Physics and Astronomy, University College London, London WC1E 6BT, UK.*

[§]*Australian Synchrotron, ANSTO, Clayton, Victoria 3168, Australia.*

[‖]*Centre for Quantum Computation and Communication Technology, School of Physics, University of Sydney, Sydney, New South Wales 2006, Australia.*

[⊥]*London Centre for Nanotechnology, University College London, London WC1H 0AH, UK.*

E-mail: s.schofield@ucl.ac.uk

Abstract

The coverage-dependent behaviour of p-methoxyacetophenone on the clean Si(001) surface was followed using X-ray photoelectron spectroscopy and supporting density functional theory calculations. Unlike other multifunctional organic molecules, this compound exhibits a high selectivity of adsorbate species formation by forming only two distinct adsorbate structures at low coverage, with a third configuration forming at high coverages. At low coverage, surface chemisorption is driven by methoxy group dissociation. However, at high coverage, the surface footprint required for this process is no longer available, leading to the formation of less thermodynamically stable adsorbates that are datively bonded to the surface with a smaller footprint. This coverage-dependent but well-defined behaviour is promising in designing functional organic-inorganic interfaces on silicon.

Introduction and background

The functionalization of semiconductor surfaces with organic adsorbates has been at the heart of designing organic-inorganic interfaces for about five decades. High reactivity, unusual surface structure, and utility in common semiconductor applications make the Si(001) surface a great model system for such studies.[1] However, despite the fact that a large number of surface reactions on silicon have been designed, understood, and controlled with high precision,[2] the selective functionalization of this surface in vacuum continues to present a number of challenges. First, the process of functionalization requires the organic molecules to be reacted to have at least two different functionalities, one of which should explicitly react with the surface and the other should be available for further processing.[3] Ideally, this approach should be driven by thermodynamic control, where the most stable surface adduct is formed. However, the problem is also in the complexity of the Si(001) surface, which is covered with rows of silicon dimers, making a number of similar surface reactions possible: e.g., across the dimer; along the dimer row; and across the trough (between two lines of

silicon dimers). In addition, the majority of surface reactions on this surface occur via the formation of weakly bonded surface intermediates, meaning that in the case of multiple functionalities and multiple adsorption sites, the formation of the final products is also affected tremendously by kinetically controlled processes.[4] Thus, new approaches and new compounds that could form selective surface adducts,[5] or manipulations of the adsorbates by processing conditions are always in demand.

This work uses experimental and computational methods to understand the adsorption of a multifunctional organic compound, namely p-methoxyacetophenone (CH_3O-C_6H_4-C(O)-OCH_3), on a clean Si(001) surface in vacuum. The choice of this compound is based on our previous investigations of acetophenone on Si(001);[6,7] but with p-methoxyacetophenone we add an additional chemical functionality that is designed to drive a specific surface reaction towards the most thermodynamically stable product at low coverage and also to allow the formation of a different surface adduct at high coverage but also with a high degree of selectivity. X-ray photoelectron spectroscopy (XPS) is used to record surface spectra of chemically adsorbed p-methoxyacetophenone, as a function of its coverage, and density functional theory calculations are used to understand and assign the recorded experimental spectra and to uncover the potential role of thermodynamic and kinetic controls in the formation of the proposed surface species as a function of coverage.

Methods

X-ray photoelectron spectroscopy

Experiments were performed on the soft X-ray beamline (SXR) of the Australian Synchrotron.[8] Samples were prepared and measured under ultrahigh vacuum (UHV) with a base pressure $< 5 \times 10^{-10}$ mbar. Silicon (001) substrates were n-type 0.04 – 0.06 Ωcm prepared by direct-current flash-annealing to 1200°C for 10 s. p-Methoxyacetophenone (Sigma Aldrich, 99%) was admitted to the vacuum chamber via a precision leak valve. The total

dose was calculated using the total chamber pressure and dose time. XPS measurements were performed in a connected UHV analysis chamber. Carbon (1s) XPS measurements were performed at a photon energy of 440 eV, while oxygen (1s) spectra were taken at 570 eV. Energy calibration was obtained subsequent to each C(1s) and O(1s) measurement by recording Si(2p) core spectra at the appropriate photon energy and setting the main component peak to 99.4 eV.[9]

Density functional theory

Density functional theory (DFT) calculations were performed using the Gaussian 09 suite of programs.[10] The surface was modeled by a $Si_{15}H_{16}$ cluster that represented two silicon dimers that share the same row, and a $Si_{21}H_{26}$ cluster that represented two silicon dimers from neighboring rows, with a trough between the dimers. Calculations were performed using the B3LYP method,[11,12] with the LANL2DZ basis set implemented for geometry optimizations, which proved to be a reliable basis set for efficient geometry optimization with minimal computational time.[13,14] The 6-311++G(d,p) basis set paired with Grimmes D3 dispersion corrections and original damping function (keyword EmpiricalDispersion=GD3) was then utilized for the single point energy calculations, with higher accuracy of the 6-311++G(d,p) basis set and the correction for dispersion forces contributing to a more accurate calculation of energy.[13–15]

The optimization of the in-row $Si_{15}H_{16}$ cluster was carried out without any constraints, while the optimization of the across-trough $Si_{21}H_{26}$ dimer was constrained as follows: silicon and hydrogen atoms representing the third layer and below were fixed using the ModRedundant input to freeze Cartesian coordinates, and layers two and above were not contrained. The contraints were implemented to simulate a solid surface of silicon, with unconstrained optimization leading to an incorrect (buckled) structure. Methoxyacetophenone adsorption on the in-row $Si_{15}H_{16}$ dimer was investigated by dative bond attachment of methoxyacetophenone on the silicon dimer through the methoxy oxygen and the ketone oxygen, with the

methoxyacetophenone molecule perpendicular to the silicon surface. Methoxyacetophenone adsorption on the across-trough $Si_{21}H_{26}$ dimer was investigated by the simultaneous dative attachment of the methoxy oxygen and the ketone oxygen, with the methoxyacetophenone molecule parallel to the silicon surface. Both strategies were used to determine the energetically favorable orientation on the surface, as well as to gain insight into the transition state for methyl cleavage from the methoxy group. Adsorption energies were calculated from total energy calculations according to the formula:

$$E_{\text{adsorption}} = E_{\text{adsorbate + substrate}} - (E_{\text{substrate}} + E_{\text{gas phase molecule}})$$

The structure of the transition state of methyl cleavage was determined using the synchronous transit-guided quasi Newton method.[16] Vibrational frequencies were calculated to confirm that this structure is a saddle point on the potential energy surface that is consistent with a methyl cleavage reaction.

Core-level energies of the surface models were calculated using Koopmans theorem, which asserts that the binding energy of single electrons is equal to their molecular orbital energy. Koopmans theorem was used to predict C (1s) and O (1s) core-level energies at the B3LYP/LANL2DZ level and the B3LYP/6-311++G(d,p) level with D3 corrections. The absolute values of binding energies were calibrated by comparison with experimental XPS binding energies reported for acetone[17] and methanol.[18,19] From this calibration, a correction term of +8.0 eV was used for C (1s) core-energy levels and +11.4 eV for O(1s) core energy levels, resulting in theoretical binding energies which were comparable to experimental values. Our calculated binding energy estimates provide valuable insight into the surface structure and orientation of methoxyacetophenone on the silicon surface when compared with our experimentally measured binding energies

XPS peak identification

In order to assign measured C(1s) XPS peaks to particular chemical species it is useful to consider prior experiments performed for molecular adsorption on Si(001). We present here a brief and non-exhaustive review of C(1s) and O(1s) peak shifts for organic adsorbates on silicon, which is summarized in Table 1. For XPS peak analysis of multifunctional adsorbates like p-methoxyacetophenone, it is useful to refer to XPS spectra of simpler adsorbates where peak assignments can be made with little ambiguity. Perhaps the simplest adsorbate is ethylene, whose adsorption was investigated by Liu and Hamers[20] who reported a single peak at 284.0 eV (full width at half maximum (FWHM) 0.9 eV). Using a synchrotron-based experimental set-up, Rochet et al.[21] reported a principal component at 284.0 eV (FWHM 0.8 eV) and a smaller peak ($< 9\%$) at 283.3 eV. Similar results (283.95 & 283.38 eV) were also reported by Yeom et al.[22] The main peak at approximately 284 eV is attributed to C-Si bonding from molecularly adsorbed ethylene in a di-σ configuration in all three reports[20–22] which is in agreement with scanning tunnelling microscopy (STM) experiments,[23,24] density functional theory calculations,[25] and results of numerous other surface analytical techniques.[26] The smaller peak at 283.3 eV was not definitively assigned, but several possible explanations were offered: this peak could be due to different chemical configurations resulting from some fraction of dissociative adsorption producing adsorbed molecular fragments, e.g., CH_2,[21] or some fraction of inter-dimer molecular adsorption.[22] Alternatively, it might be attributed to vibrational fine structure; the gas phase spectrum involves a 400 meV peak shift due to C-H vibrational stretch modes and similar shift for the adsorbed molecule would produce a peak as observed in the XPS data.[21,22]

Other organic molecules containing only carbon atoms whose adsorption to Si(001) has been investigated with XPS include acetylene,[20,22] cyclopentene,[20,27] benzene,[28] and C_{60}.[29] In each case, a peak at or very near (within 0.3 eV) 284.0 eV was attributed to carbon bonded to silicon (Si-C) in agreement with the ethylene results discussed above. Likewise, the dissociative adsorption of methyl iodide resulting in surface-bound CH_3 gave a single

component peak at 284.1 eV.[30] In addition to the 284.3 eV peak assigned above to Si-C bonding, a peak at 284.8 eV was attributed to C-C bonding for adsorbed cyclopentene,[20,27] and a peak at 284.2 eV was attributed to C=C bonding in the case of benzene adsorption.[28] In the case of C_{60}, the major peak component corresponding to the bulk of the molecule (i.e., not involved with bonding to silicon) was found at 285.3 eV for intermediate coverage that shifted to 284.5 eV for monolayer coverage.[29]

In cases where surfaces are annealed after dosing, it has been reported that Si-C peak energies shift to lower energies (282.6 – 283.4 eV) attributed to increasingly strong Si-C bonding.[21,30] For sufficiently high annealing temperatures the formation of silicon carbide-like alloy products are observed with similar low binding energies, e.g., 282.8 eV.[21]

The adsorption of oxygen containing molecules has also been studied, e.g., ref.[31] reports the adsorption of methanol, 1,2-cyclohexanedione (CHD) and 9,10-phenanthrenequinone (PQ) to Si(001). Here, C(1s) peaks attribute to C=C bonding were reported at 284.4, 284.6 and 285 eV, while peaks assigned to Si-O-C were reported at 286.6, 286.0, and 285.8 eV. For each of these three adsorbates, oxygen (1s) spectra exhibited a single component between 532.3 and 532.5 eV attributed to C-O-Si. The adsorption of phenol was investigated in ref.[32] where similar C(1s) and O(1s) peak energies were observed at 285.1, 286.6, and 532.5 eV with corresponding assignments to ref.[31] Methanol adsorption was revisited in ref.[33], where single component spectra were found at 286.6 and 532.2 eV, attributed to C-O and C-O-Si, respectively.

Particularly interesting for the present work are XPS measurements of monolayers and multilayers of acetaldehyde and acetone on Si(001) reported in ref.[17]: for multilayer coverage (cryogenic temperature deposition) they found a peak at 532.7 eV, attributed to unreacted C=O. For monolayer coverages, two peaks, at 532.5 and 531.5 eV, were reported. Similarly to the discussion presented above, the 532.5 eV peak can be readily assigned to Si-C-O bonding. The adsorption structures for acetone[34,35] and acetaldehyde[36] have been determined via a combination of DFT and STM and are known to form 4 and 5 membered ring structures

involving Si-O-C bonds on Si(001). Thus the 531.5 eV peak must also correspond to Si-C-O, but in a different structural configuration. Consideration of the various structures discussed above leads to the conclusion that oxygen in the strained [2+2] Si-Si-O-C cycloaddition configuration gives rise to the peak for adsorbed acetaldehyde and acetone peaks at 531.5 eV.

In addition to chemical shifts, there are also small and systematic electrostatic peak shifts due to band bending. Silicon is less electronegative than both carbon and oxygen, and because of this there is typically some redistribution of negative charge from the surface to the adsorbate. This induces an upward band-bending at the silicon surface and a shift of the measured adsorbate XPS peaks to higher binding energies. The observed shifts increase with the molecular coverage and are typically in the range of 0.1 to 0.3 eV for high coverages.[20,21,28,37,38]

This brief overview allows for placing a number of starting constraints on the assignment of the XPS features described below for adsorption of p-methoxyacetophenone as a function of coverage. It also serves as a useful experiment-based confirmatory cross-check on the calculated binding energies for our structures based on DFT simulations that we present below.

Results and Discussion

Measurement and analysis of O(1s) and C(1s) X-ray photoelectron peaks

Oxygen 1s XPS spectra of Si(001) surfaces exposed in vacuum to p-methoxyacetophenone are shown in Fig. 1a. Each spectrum was acquired from a sample that was first flash annealed to produce an atomically-clean Si(001) surface and then dosed with p-methoxyacetophenone at doses of 0.18 to 9 L as indicated. At the lowest coverage (0.18 L), we identify in the O(1s) spectra two peaks at 531.4 and 532.1 eV (Fig. 1a), which compare favorably to the 531.4 and 532.5 eV peaks reported in ref.[17] for adsorption of acetaldehyde and acetone to Si(001). It

is therefore tempting to assign the two peaks in our O(1s) spectra to Si-O-C bonding: e.g., the largest component peak at 532.1 eV could be assigned to oxygen directly bonded to the silicon in a similar manner as observed for methanol, phenol, etc.[3,32,39] (see also Table. 1). By analogy to acetaldehyde and acetone,[17,34,36] it might also be tempting to assign the 531.4 eV peak to Si-O-C bonding in a strained configuration. However, the additional complexity of the p-methoxyacetophenone molecule may also provide alternative assignments for the two peaks we observe here at low coverage and we defer definitive assignment of these peaks to the discussion below where we introduce DFT simulation data of O(1s) binding energies for p-methoxyacetophenone adsorbed in different configurations on Si(001). For the highest exposure (9 L) we find an additional peak in our experimental spectra at 533.5 eV. Comparing to the multilayers of acetaldehyde and acetone formed at cryogenic temperatures[17] suggests that this may be due to unreacted carbonyl (C=O) at high coverages. It should be noted that at the temperature of the experiments performed here, multilayer formation is not expected (e.g., see previous studies of similar compounds on silicon[17,34]), so all the features observed correspond to the formation of strongly adsorbed monolayers.

In the C(1s) spectra in Fig. 1b, at high coverage we find peaks at 283.8, 284.7, 285.7, and 286.5 eV. These peaks are shifted by 0.2 eV compared to their positions at low coverage, which we attribute to electrostatic effects as previously observed for organic monolayers deposited on silicon.[20,21,28,37,38] There is also an additional peak at 287.4 eV that occurs only for the high coverage surface. Comparison to the literature (see Table 1) suggests that the lowest and highest binding energies can be assigned to C-Si bonding (283.8 eV) and carbonyl C=O (287.4 eV), respectively. The dominant peak in all spectra is the 284.7 eV peak, and for that reason and by analogy with the literature we can assign this peak to C-C and C=C bonding within the adsorbate. This peak is also slightly broader than the other peaks (full width half maximum $\sim$ 1 eV) reflecting the expected heterogenous broadening due to the differences in bonding geometry of the carbon-carbon bonds in the adsorbates. We anticipate bonding of the adsorbate to silicon via the oxygen atoms, and for this reason

and by comparison to literature we can assign the 286.5 eV peak to Si-O-C bonding.

The remaining unassigned peak at 285.7 eV could equally well be assigned to C=C or C-O bonding considering the literature values in Table 1. To make a determination we look at the percentage of the peak areas with respect to the total area of all the peaks. If the 285.7 eV peak is assigned to C=C bonding, then the peaks that do not involve any bonding to oxygen are 283.8 eV, 284.7 eV, and 285.7 eV. Summing the areas of these peaks gives a percentage composition of $> 80\%$ for all doses. However, this is inconsistent with the composition of p-methoxyacetophenone, which has 9 carbon atoms, 3 of which involve bonding to oxygen and 6 of which do not. Therefore, we attribute the 285.7 eV to Si-O-C species. This means that both the 285.7 and 286.5 eV peaks are assigned to Si-O-C bonding, but with local variation in their character. This is consistent with the assignment of the O(1s) peaks above, where we also found two Si-O-C peaks at energies 531.3 and 532.2 eV. A summary of the measured peak energies in our data, the assigned chemical structures, and literature references with similar assignments for comparison are provided in Table 2.

Variation of peak area with dose

The variation of peak areas with dose for both C(1s) and O(1s) spectra are shown in Fig. 2. The variation of C(1s) peaks up to 9 L is shown in Fig. 2a, with an expansion of the region up to 1 L shown in the inset. As clearly seen in the inset to Fig. 2a, up to 1 L there is a uniform increase in the area of all peaks other than C=O with the relative ratio of the peaks remaining constant throughout. After 1 L there is a distinct change: the overall increase of all peaks slows considerably and there is no further increase in the 285.7 eV peak assigned to Si-O-C. After 4.5 L we see an increase in the 287.4 eV peak assigned to C=O. In Fig. 2b we plot the C(1s) peak areas as a percentage of the total. Gray open circles in Fig. 2b show the addition of the three peaks involving bonding to oxygen (i.e., 285.7, 286.5, and 287.4 eV), and we see that to within our uncertainties we have 1/3 carbon bonded to oxygen and 2/3 carbon not bonded to oxygen, consistent with the expected ratio from the composition of

the p-methoxyacetophenone molecule.

Analogous data for peak areas for the O(1s) spectra are shown in Fig. 2c, with the relative percentage of each peak shown on a linear-log plot in Fig. 2d. Comparing the relative ratios of the two main observed features we see that the initial ratio of the two features is approximately 3 to 1 for the 532.1 eV peak intensity compared to that of the 531.4 eV peak, which decreases to around 1.5 for exposures approaching 4.5 L (see inset to Fig. 2d). Above this exposure, the formation of a high binding energy feature around 534 eV is observed; as discussed above, this can be assigned to the emergence of C=O in the spectra in agreement also with the onset of carbonyl C=O in the C(1s) spectra above 4.5 L. This analysis will be used below, once the positions of the binding energy features have been clarified with the help of computational investigations.

At exposures below 1 L the adsorption is nearly linear with exposure, suggesting high adsorption coefficient. However, for higher exposures there is a deviation from linearity, indicating a substantial decrease in adsorption coefficient, which would be consistent with fewer appropriate adsorption sites available on a surface at high coverage.

Possible reaction pathways and adsorption energy calculations

To aid in the interpretation of the observed experimental data we turn to DFT calculations. The number of possible configurations of p-methoxyacetophenone on the Si(001) surface is very large and this prohibits an exhaustive set of total energy calculations for all possible configurations. It is therefore prudent to apply chemical intuition drawn from prior investigations of molecular adsorption on the Si(001) surface to narrow the scope of calculated structures. Prior work has shown that a common route to the attachment of organic molecules to Si(001) is via the formation of a dative bond between a lone pair and an electrophilic down-buckled silicon atom.[6,7,34,40] Considering the structure of p-methoxyacetophenone, it is reasonable to expect that this molecule may attach via either of the two oxygen atoms, i.e., belonging to the ketone and methoxy functional groups at each end of the molecule. Below,

we outline two main reaction pathways that we will show can account for the observed experimental data. For each structure we have calculated the adsorption energy, which is given in Table 3. The cluster model structures were first optimised using the B3LYP-D3/LANL2DZ approach to determine the geometry and subsequently a single-point energy calculation of the optimised structure was performed using B3LYP-D3/6-311++G(d,p) computation.

Pathway 1: shown in Figure 3a follows ketone attachment. It illustrates a reaction pathway involving attachment via the ketone that is drawn in direct analogy with the established reaction path for acetophenone on Si(001).[6,7] Here, a dative bond is first formed between the ketone and a surface silicon atom to form the dative ketone with a calculated adsorption energy of -1.32 eV. This structure can be stabilised via a hydrogen shift to the surface resulting in the formation of a C=C double bond and a terminal CH_2 group. By analogy with previous work[6,7] we anticipate this structure will be unstable with respect to further reaction of the CH_2 group with the surface silicon to form the "intermediate" with an adsorption energy of -2.54 eV. In the case of acetophenone[6,7] the analogous intermediate structure was found to convert to an allyl structure in which two additional Si-C bonds are formed between the phenyl ring and the substrate. The analogous allyl structure for p-methoxyacetophenone is shown in Fig. 3a. For acetophenone it was found using the combination of experimental measurements and theoretical calculations,[6,7] that each of the transition barriers separating stages of this sequence leading to the allyl structure could be overcome at room temperature and the resulting allyl structure occurred preferentially upon deposition at room temperature. Due to the similarity of acetophenone and p-methoxyacetophenone, it might be anticipated that this sequence will also occur for p-methoxyacetophenone. However, the presence of the methoxy group for p-methoxyacetophenone also suggests the possibility of this pathway being diverted prior to the formation of the allyl structure due to the possibility of reaction via the methoxy oxygen.

Pathway 2: shown in Fig. 3b follows attachment via dissociation of methoxy group. Here, a dative bond is formed between the methoxy and a down-buckled silicon atom, pro-

ducing a structure with a formation energy of just −0.77 eV. This configuration can then further stabilise via the cleavage of the C-O bond and methyl group transfer to the surface, producing a remarkable energy stabalization to produce the "methyl cleavage" structure with an adsorption energy of −3.63 eV. We note that a recent report of diethylether adsorption on ref.[41,42] showed a similar dissociatiative pathway involving cleavage of C-O, and that this was observed to occur well below room temperature, in fact just above 100 K (calculated transition energies were reported in Ref.[43]).

It can perhaps also be expected that some combination of the above pathways might occur. Given that the separation between oxygen atoms in the p-methoxyacetophenone molecule is $\sim$ 7 Å, we might anticipate bonding to corresponding atoms across two silicon dimer rows (separation 7.6 Å). Attachment of the molecule to the surface via both the methoxy and the ketone oxygen results in the "across-trough dative" structure shown in Fig. 3c. Because the adsorbate is also spanning across one silicon dimer, there is also the formation of a strong bond between one of the phenyl carbon atoms and a surface silicon atom, similar to the attachment seen in the allyl structure. The across-trough dative structure was found to have an adsorption energy of −2.36 eV. Further stabilisation of this structure is possible via methyl cleavage, analogous to that in pathway 2, which leads to the "across-trough methyl-cleavage" structure shown in Fig. 3d. This was by far the most energetically favourable configuration in our investigation with an adsorption energy of −5.18 eV.

Carbon peak ratio considerations

At the low coverage regime (below 1 L exposure in Fig. 1), the use of the peak fitting described above yields the following values for the contribution of carbon-containing species on silicon to the observed spectra: 5% correspond to C-Si, 60% - C-C/C=C, 16% C-O-Si (type 1) and 19% of C-O-Si (type 2). If the allyl-type species (Fig. 3a), proposed as the major contributor to the acetophenone attachment to the Si(001) surface, were the major species observed in the present investigation of p-methoxyacetophenone, then the contribution of the

C-Si species to the spectra would be expected to be 3/9 (or 1/3 of intensity), which is clearly not the case. For the other stable attachment configurations (methyl cleavage, across-trough species; Fig. 3c, 3d), the expected ratios of the observed and predicted features would be approximately similar to the experiments. Given the stability comparison in Table 3 and the argument that methyl cleavage is not kinetically hindered, four possible types of surface species might be expected to contribute to binding of p-methoxyacetophenone to the Si(001) surface: direct methyl cleavage (−3.63 eV; Fig. 3b), adsorption across the trough followed by methyl cleavage (−5.18 eV; Fig. 3d), Intermediate (−2.54 eV; Fig. 3a), and doubly datively bonded structures, where no dissociation occurs but both O atoms are in a direct contact with the surface silicon atoms (−2.36 eV; Fig. 3c). None of these structures can be ruled out based on the approximate analysis performed above for the allyl intermediate. We must therefore include additional considerations in for the assignment of our spectral features.

Kinetic considerations

Thermodynamic considerations alone would suggest a preference for the formation of the most favourable structures. However, despite the substantial thermodynamic driving force, it is possible that high barriers, e.g., for methyl cleavage, could prevent the formation of the most stable products. By comparison with previous works for organic attachment to silicon we can anticipate the kinetic barriers to dative adsorption are very small and easily overcome at room temperature.[7,35,40] Of the various transitions in Fig. 3, the next smallest barrier is likely to be the H shift reaction in the initial stages of pathway 1 and likewise comparison to previous work suggests this barrier will be easily overcome at room temperature, leading us to conclude that adsorption of p-methoxyacetophenone to Si(001) may rapidly progress via dative bonding and H shift reaction to form the across-trough dative structure shown in Fig. 3c. Full calculation of the kinetic barriers for our suggested pathways is outside the scope of this work due to the complexity of the adsorbate and the large number of possible transition states between each of these structures. Nevertheless, due to its importance in the

determination of possible adsorbate configurations, we have attempted to address the barrier for methyl cleavage. A transition state for methyl cleavage from the across-trough dative structure was evaluated and the barrier for the process was found to be 1.0 eV (99.2 kJ/mol) (see Supplementary Fig. S1). This suggests that methyl dissociation can occur kinetically at room temperature, which is supported by the recent report of C-O cleavage in diethylether adsorption on on Si(001).[41] Thus, a p-methoxyacetophenone adsorbate having reached the across-trough dative structure (−2.36 eV) may dramatically increase its stability via methyl cleavage to the across-trough methyl-cleaveage structure (Fig. 3d; −5.18 eV), provided that sufficient space remains available for these processes to occur. The barrier to methyl cleavage from the dative methoxy structure might be expected to be similarly overcome at room temperature so that the methyl cleavage structure is also possible for room temperature dosed surfaces.

Simulated O(1s) binding energies

Given the range of possible structures (Fig. 3) and the fact that each one of these structures contains two oxygen atoms, it is striking that the measured O(1s) spectra show only two components for almost all doses. This suggests that it may be possible to provide assignments for the spectral features via simulation of O(1s) binding energies. We have calculated the O(1s) binding energies for each of the structures shown in Fig. 3; the calculated binding energies are shown in Fig. 4, and are tabulated in Supplementary Table S1. The range of predicted O(1s) binding energies is broad, spanning almost 5 eV in stark contrast to the experimental data. This confirms that only a very limited subset of structures can be giving rise to our observed experimental features. From the predicted O(1s) binding energies for the four possible dominant surface species we find that the methyl-cleavage structure and the across-trough methyl-cleavage structure are both predicted by our DFT simulations to produce XPS peaks observed experimentally. Specifically, the methyl cleavage structure is predicted to exhibit two peaks at 531.3 and 532.6 eV, and the structure bound across the

silicon trough followed by methyl cleavage should produce two very closely spaced features at 532.0 and 532.1 eV. In other words, if these structures are formed at low coverage in equimolar amounts on a surface, they would produce the experimentally observed spectrum, to within the accuracy of the calculations, with one O(1s) peak above 532 eV being about three times as intense as the feature at 531.5 eV. At higher coverage, the number of surface sites that could accommodate doubly bound p-methoxyacetophenone followed by a methyl cleavage decreases, meaning that if the spectra recorded are dominated by those two species, the ratio between the two features would be expected to decrease toward 1:1, which is what is observed experimentally (see inset to Fig. 2d for coverages up to 4.5 L).

What about the other two possible stable surface structures: the intermediate and the across-trough dative structures? In addition to being less stable than the structures with methyl cleavage, they are also expected to give rise to the experimental O(1s) features above 533 eV, which is not observed at low coverage. Thus, analysis of the experimental spectra indicates that the low coverage surface exhibits a mixture of the the methyl-cleavage and the across-trough methyl-cleavage structures. The details of the kinetic barrier separating these two structures and preventing the methyl-cleavage structure adsorbates from converting to the more stable across-trough methyl-cleavage structure is not known and is beyond the scope of this paper; however, it might be anticipated that further work, e.g., atomic-resolution scanning tunnelling microscopy, can provide insight, especially if combined with a more exhaustive set of kinetic barrier calculations.

At high exposures, above 4.5 L, a new peak at 533.5 eV is observed. It is likely at these high coverages that there is insufficient space to accommodate the intermediate, or the across-trough bonding species which all have large footprints requiring 3 or 4 reactive silicon sites across at least two silicon dimers. The number of sites large enough to accommodate these species will decrease rapidly as the coverage increases. However, the availability of sites with one or two reactive silicon atoms will remain finite up until the point where the surface is completely saturated. Effects related to molecular footprint, stiffness of backbone, and

geometric fit to surface reactive sites have been extensively explored on the germanium (001) surface by the Bent group.[44–46] In contrast, the dative ketone and dative methoxy species both have relatively small footprints and are also both predicted by our DFT simulations to give rise to XPS features at binding energies above 533 eV. Thus, at high coverage a direct adsorption with either ketone functionality (dative ketone) or methoxy group functionality (dative methoxy) could take place despite the fact that these two types of structures are substantially less stable than the intermediate or across-trough dative structures. Of the two structures, the weakest-bound structure (dative methoxy; -0.77 eV) is predicted to yield the highest binding energy peak at 535 eV, while the more strongly bonded structure (dative ketone; -1.32 eV) produces two closely spaced features at 533.8 and 534.0 eV (see Supplementary Table S1). Therefore, consideration of the O(1s) simulated spectra suggests that the dative ketone produces a better fit to the observed experimental data. However, while the DFT predicted XPS binding energies can be expected to produce qualitative agreement with experiment, differences in adsorbate/substrate charge transfer etc. compared to a real system can be expected to produce quantitative differences. We therefore do not immediately rule out the dative methoxy structure based on the predicted too-high O(1s) carbonyl-derived peak and instead turn to the analysis of the C(1s) specra.

Simulated C(1s) binding energies

The full assignment of all the predicted C(1s) features for the structural models shown in Fig. 3 are provided in Supplementary Table S2 and we find good qualitative and systematic agreement with the literature-based assignments discussed at the beginning of the results section above. Figure 5 shows simulated XPS spectra based on the calculated binding energies for a selection of the structures starting with the gas phase p-methoxyacetophenone (Fig. 5a), the two structures that we believe form on the surface at low coverage, i.e., the across-trough methyl-cleavage structure (Fig. 5b), the methyl cleavage structure (Fig. 5c), and the two datively bonded structures: the dative ketone (Fig. 5d) and dative methoxy

(Fig. 5e). The predicted C(1s) binding energies for these structures are very much consistent with the analysis presented above based on the O(1s) components: The two low coverage species produce a principal component that peaks just below 285 eV with also a smaller component at higher binding energy. Importantly, the higher binding energy component for the two structures differ by about 0.8 eV, such that the addition of these two spectra is expected to produce a principal component just below 285 eV with two side peaks at higher binding energy, which is what is observed in the experimental spectra for all doses except the 9 L dose (See Fig. 1).

For the highest dose, both the dative ketone and the dative methoxy species produce a principal component around 286 eV with one or two additional features occurring above 287 eV. If we compare to the experimental data, we see that there is a continued growth in the 286.5 eV peak at the 9 L dose. We can therefore reasonably assume that the principal component of the datively bound species is the reason for this continued increase in the experimental spectra. Note that this implies that the principal component of the simulated dative structured (Figs. 5d and 5e) should overlap with the side peak of the methyl cleavage structure (Fig. 5c). This is not quite the case for our simulations, but we suggest this is a result of an overall shift of the two simulated spectra as mentioned above, which most probably arises due to charge transfer to the substrate not being properly accounted for in the cluster model calculations. Notwithstanding this small discrepancy, the two dative bonded structures provide good explanation for the experimental measurement for the 9 L dose: both the dative ketone and the dative methoxy produce a pair of binding energies above 287 eV that can account for the observation of a 287.4 eV peak in the 9 L dose experimental spectrum. The fit to experiment is best for the dative methoxy species, where the Gaussian smearing results in the two binding energies appearing as a single peak component at at 287.6 eV. In contrast, the fit to experiment is reasonable for the dative ketone, but in this case some additional explanation is required for the slightly larger separation between the two highest energy peaks in this spectrum for which the Gaussian smearing we have employed

is insufficient for these two components to appear as a single peak.

Conclusion

This work describes the unique coverage-dependent behaviour of p-methoxyacetophenone on a clean Si(001) surface observed by XPS and supported by DFT investigations. Several chemical functionalities available in this molecule would normally imply that a large number of surface structures would be observed experimentally; however, in this case, the presence of methoxy functional group appears to steer the reaction towards CH_3-O dissociation and govern the distribution of surface species upon adsorption. Assigning the peaks observed in XPS and following their evolution as a function of coverage suggests that at low coverage the most thermodynamically stable surface species are formed following CH_3-O dissociation; i.e., the two structures we have labelled "methyl-cleavage" and "across-trough methyl-cleaveage". However, as the surface coverage increases, the footprint of the remaining surface sites required for their formation becomes unavailable, and more weakly bound species are also formed. Specifically, the unique structure of the p-methoxyacetophenone molecule offers a possibility of stable datively bonded species to be formed, with dative bonding through either the methoxy or the ketone groups producing similarly predicted spectroscopic features in our simulations such that we cannot say which is preferred or rule out the possibility that both form in some fraction. This unusual behaviour, with high selectivity at low coverage and a different selectivity at high coverage, can be used to design a variety of organic inorganic interfaces on silicon surfaces as a function of surface concentration of a multifunctional adsorbate.

Supporting Information

The Supporting Information is available free of charge on the ACS Publications website at DOI: 10.1021/acs.jpcc....

Figure: Computationally predicted reaction pathway for adsorption of methoxyacetophenone across the trough of the silicon dimers followed by dissociation of the methoxy group.

Tables: Calculated O(1s) and C(1s) binding energies. Cartesian (xyz) coordinates for all computed structures.

In addition, all the data created during this research are openly available via zenodo.org at

https://doi.org/10.5281/zenodo.2650188

Acknowledgements

Part of this research was undertaken at the soft X-ray (SXR) beamline of the Australian Synchrotron, part of ANSTO. This work was supported by the Engineering and Physical Sciences Research Council (EP/L002140/1) and the National Science Foundation (CHE 1057374). XPS peak fitting was performed using CasaXPS 2.3.16 (http://www.casaxps.com/). Marvin 15.6.29 was used for drawing chemical structures and reactions (http://www.chemaxon.com).

Data accessibility

References

(1) Teplyakov, A. V.; Bent, S. F. Semiconductor surface functionalization for advances in electronics, energy conversion, and dynamic systems. *J. Vac. Sci. Technol. A* **2013**, *31*, 050810.

(2) Leftwich, T. R.; Teplyakov, A. V. Cycloaddition reactions of phenylazide and benzylazide on a Si (100)-2 $\times$ 1 surface. *J. Phys. Chem. C* **2008**, *112*, 4297–4303.

(3) Länger, C.; Heep, J.; Nikodemiak, P.; Bohamud, T.; Kirsten, P.; Höfer, U.; Koert, U.; Dürr, M. Formation of Si/organic interfaces using alkyne-functionalized cyclooctynes–

precursor-mediated adsorption of linear alkynes versus direct adsorption of cyclooctyne on Si(001). *J. Phys.: Condens. Matter* **2019**, *31*, 034001.

(4) Leftwich, T.; Teplyakov, A. V. Chemical manipulation of multifunctional hydrocarbons on silicon surfaces. *Surf. Sci. Rep.* **2007**, *63*, 1–71.

(5) Reutzel, M.; Münster, N.; Lipponer, M. A.; Länger, C.; Höfer, U.; Koert, U.; Dürr, M. Chemoselective reactivity of bifunctional cyclooctynes on Si(001). *J. Phys. Chem. C* **2016**, *120*, 26284–26289.

(6) O'Donnell, K. M.; Warschkow, O.; Suleman, A.; Fahy, A.; Thomsen, L.; Schofield, S. R. Manipulating the orientation of an organic adsorbate on silicon : a NEXAFS study of acetophenone on Si(001). *J. Phys.: Condens. Matter* **2015**, *27*, 054002.

(7) Schofield, S. R.; Warschkow, O.; Belcher, D. R.; Rahnejat, K. A.; Radny, M. W.; Smith, P. V. Phenyl attachment to Si(001) via STM manipulation of acetophenone. *J. Phys. Chem. C* **2013**, *117*, 5736–5741.

(8) Cowie, B. C. C.; Tadich, A.; Thomsen, L. The current performance of the wide range (90-2500 eV) soft x-ray beamline at the Australian Synchrotron. *AIP Conf. Proc.* **2010**, *1234*, 307–310.

(9) Gallet, J. J.; Bournel, F.; Rochet, F.; Köhler, U.; Kubsky, S.; Silly, M. G.; Sirotti, F.; Pierucci, D. Isolated silicon dangling bonds on a water-saturated n^+-doped Si(001)-2$\times$1 surface: An XPS and STM study. *J. Phys. Chem. C* **2011**, *115*, 7686–7693.

(10) Frisch, M. J.; Trucks, G. W.; Schlegel, H. B.; Scuseria, G. E.; Robb, M. A.; Cheeseman, J. R.; Montgomery, Jr., J. A.; Vreven, T.; Kudin, K. N.; Burant, J. C. et al. GAUSSIAN 03, Revision E.01 (Gaussian, Inc., Wallingford CT). 2004.

(11) Becke, A. D. Density-functional thermochemistry. III. The role of exact exchange. *J. Chem. Phys.* **1993**, *98*, 5648–5652.

(12) Lee, C.; Yang, E.; Parr, R. G. Development of the Colic-Salvetti correlation-energy formula into a functional of the electron density. *Phys. Rev. B* **1988**, *37*, 37785.

(13) McLean, A. D.; Chandler, G. S. Contracted Gaussian basis sets for molecular calculations. I. Second row atoms, Z=11-18. *J. Chem. Phys.* **1980**, *72*, 5639–5648.

(14) Krishnan, R.; Binkley, J. S.; Seeger, R.; Pople, J. A. Self-consistent molecular orbital methods. XX. A basis set for correlated wave functions. *J. Chem. Phys* **1980**, *72*, 650.

(15) Grimme, S.; Antony, J.; Ehrlich, S.; Krieg, H. A consistent and accurate ab initio parametrization of density functional dispersion correction (DFT-D) for the 94 elements H-Pu. *J. Chem. Phys.* **2010**, *132*, 154104.

(16) Peng, C.; Schlegel, H. B. Combining synchronous transit and quasi-Newton methods to find transition states. *Isr. J. Chem.* **1993**, *33*, 449–454.

(17) Armstrong, J. L.; White, J. M. Thermal decomposition reactions of acetaldehyde and acetone on Si(100). *J. Vac. Sci. Tech. A* **1997**, *15*, 1146–1154.

(18) Sexton, B. A.; Rendulic, K. D.; Hughes, A. E. Decomposition pathways of $C_1 - C_4$ alcohols adsorbed on platinum (111). *Surf. Sci.* **1982**, *121*, 181–198.

(19) Rodriguez De La Fuente, O.; Borasio, M.; Galletto, P.; Rupprechter, G.; Freund, H.-J. The influence of surface defects on methanol decomposition on Pd(111) studied by XPS and PM-IRAS. *Surf. Sci.* **2004**, *566-568*, 740.

(20) Liu, H.; Hamers, R. J. An X-ray photoelectron spectroscopy study of the bonding of unsaturated organic molecules to the Si(001) surface. *Surf. Sci.* **1998**, *416*, 354–362.

(21) Rochet, F.; Jolly, F.; Bournel, F.; Dufour, G.; Sirotti, F.; Cantin, J.-L. Ethylene on Si(001)-2 $\times$ 1 and Si(111)-7 $\times$ 7: X-ray photoemission spectroscopy with synchrotron radiation. *Phys. Rev. B* **1998**, *58*, 11029–11042.

(22) Yeom, H. W.; Baek, S. Y.; Kim, J. W.; Lee, H. S.; Koh, H. Adsorption of C_2H_2 and C_2H_4 on Si(001): core-level photoemission. *Phys. Rev. B* **2002**, *66*, 1–6.

(23) Li, L.; Tindall, C.; Takaoka, O.; Hasegawa, Y.; Sakurai, T. STM study of C_2H_2 adsorption on Si(001). *Phys. Rev. B* **1997**, *56*, 4648–4655.

(24) Harikumar, K. R.; Polanyi, J. C.; Zabet-Khosousi, A.; Czekala, P.; Lin, H.; Hofer, W. A. Directed long-range molecular migration energized by surface reaction. *Nat. Chem.* **2011**, *3*, 400–408.

(25) Pan, W.; Zhu, T.; Yang, W. First-principles study of the structural and electronic properties of ethylene adsorption on Si(100)-(2×1) surface. *J. Chem. Phys.* **1997**, *107*, 3981.

(26) Wolkow, R. A. Controlled molecular adsorption on silicon. *Annu. Rev. Phys. Chem.* **1999**, *50*, 413–441.

(27) Khaliq, A.; Pierucci, D.; Tissot, H.; Gallet, J. J.; Bournel, F.; Rochet, F.; Silly, M.; Sirotti, F. Ene-like reaction of cyclopentene on Si(001)-2×1: An XPS and NEXAFS study. *J. Phys. Chem. C* **2012**, *116*, 12680–12686.

(28) Kim, Y. K.; Lee, M. H.; Yeom, H. W. Coverage-dependent adsorption behavior of benzene on Si(100): A high-resolution photoemission study. *Phys. Rev. B* **2005**, *71*, 115311.

(29) Cheng, C.-P.; Pi, T.-W.; Ouyang, C.-P.; Wen, J.-F. Chemisorption of C_{60} on the Si(001)-2×1 surface at room temperature. *J. Vac. Sci. Technol. B* **2005**, *23*, 1018.

(30) Cao, X.; Hamers, R. J. Silicon surfaces as electron acceptors: dative bonding of amines with Si(001) and Si(111) surfaces. *J. Am. Chem. Soc.* **2001**, *123*, 10988–10996.

(31) Fang, L.; Liu, J.; Coulter, S.; Cao, X.; Schwartz, M. P.; Hacker, C.; Hamers, R. J.

Formation of π-conjugated molecular arrays on silicon (001) surfaces by heteroatomic Diels-Alder chemistry. *Surf. Sci.* **2002**, *514*, 362–375.

(32) Casaletto, M. P.; Carbone, M.; Piancastelli, M. N.; Horn, K.; Weiss, K.; Zanoni, R. A high resolution photoemission study of phenol adsorption on Si(100)2 $\times$ 1. *Surf. Sci.* **2005**, *582*, 42–48.

(33) Länger, C.; Bohamud, T.; Heep, J.; Glaser, T.; Reutzel, M.; Höfer, U.; Dürr, M. Adsorption of Methanol on Si(001): Reaction Channels and Energetics. *J. Phys. Chem. C* **2018**, acs.jpcc.8b04583.

(34) Schofield, S. R.; Saraireh, S. A.; Smith, P. V.; Radny, M. W.; King, B. V. Organic bonding to silicon via a carbonyl group: new insights from atomic-scale images. *J. Am. Chem. Soc.* **2007**, *129*, 11402–11407.

(35) Warschkow, O.; Gao, I.; Schofield, S. R.; Belcher, D. R.; Radny, M. W.; Saraireh, S. A.; Smith, P. V. Acetone on silicon (001): ambiphilic molecule meets ambiphilic surface. *Phys. Chem. Chem. Phys.* **2009**, *11*, 2747–2759.

(36) Belcher, D. R.; Schofield, S. R.; Warschkow, O.; Radny, M. W.; Smith, P. V. Carbonyl mediated attachment to silicon: acetaldehyde on Si(001). *J. Chem. Phys.* **2009**, *131*, 104707–8.

(37) Wang, S.; He, J.; Zhang, Y.; Xu, G. Q. Adsorption of O_2 and CO_2 on the Si(111)-7$\times$ surfaces. *Surf. Sci.* **2012**, *606*, 1387–1392.

(38) Vilan, A.; Cahen, D. How organic molecules can control electronic devices. *Trends Biotechnol.* **2002**, *20*, 22–29.

(39) Soubiron, T.; Vaurette, F.; Nys, J.; Grandidier, B.; Wallart, X.; Stiévenard, D. Molecular interactions of PTCDA on Si(100). *Surf. Sci.* **2005**, *581*, 178–188.

(40) Warschkow, O.; Curson, N. J.; Schofield, S. R.; Marks, N. A.; Wilson, H. F.; Radny, M. W.; Smith, P. V.; Reusch, T. C. G.; McKenzie, D. R.; Simmons, M. Y. Reaction paths of phosphine dissociation on silicon (001). *J. Chem. Phys.* **2016**, *144*, 014705.

(41) Reutzel, M.; Mette, G.; Stromberger, P.; Koert, U.; Dürr, M.; Höfer, U. Dissociative adsorption of diethyl ether on Si(001) studied by means of scanning tunneling microscopy and photoelectron spectroscopy. *J. Phys. Chem. C* **2015**, *119*, 6018–6023.

(42) Reutzel, M.; Lipponer, M.; Dü, M.; Hö, U. Bindinge energy and dissociation barrier: experimental determination of the key parameters of the potential energy curve of diethyl ether on Si(001). *J. Phys. Chem. Lett* **2015**, *6*, 3975.

(43) Pecher, L.; Laref, S.; Raupach, M.; Tonner, R. Ethers on Si(001): a prime example for the common ground between surface science and molecular organic chemistry. *Angew. Chemie - Int. Ed.* **2017**, *56*, 15150–15154.

(44) Sandoval, T. E.; Bent, S. F. Adsorption of homotrifunctional 1,2,3-benzenetriol on a Ge(100)-2 $\times$ 1 surface. *Langmuir* **2017**, *33*, 8716–8723.

(45) Shong, B.; Brogaard, R. Y.; Sandoval, T. E.; Bent, S. F. Coverage-dependent adsorption of bifunctional molecules: Detailed insights into interactions between adsorbates. *J. Phys. Chem. C* **2014**, *118*, 23811–23820.

(46) Sandoval, T. E.; Bent, S. F. Adsorption of homotrifunctional 1,2,3-benzenetriol on a Ge(100)-2 $\times$ 1 surface. *Langmuir* **2017**, *33*, 8716–8723.

(47) Zhao, J.; Gao, F.; Pujari, S. P.; Zuilhof, H.; Teplyakov, A. V. Universal calibration of computationally predicted N 1s binding energies for interpretation of XPS experimental measurements. *Langmuir* **2017**, *33*, 10792–10799.

(48) Leftwich, T. R.; Teplyakov, A. V. Calibration of computationally predicted N 1s binding energies by comparison with X-ray photoelectron spectroscopy measurements. *J. Electron Spectros. Relat. Phenomena* **2009**, *175*, 31–40.

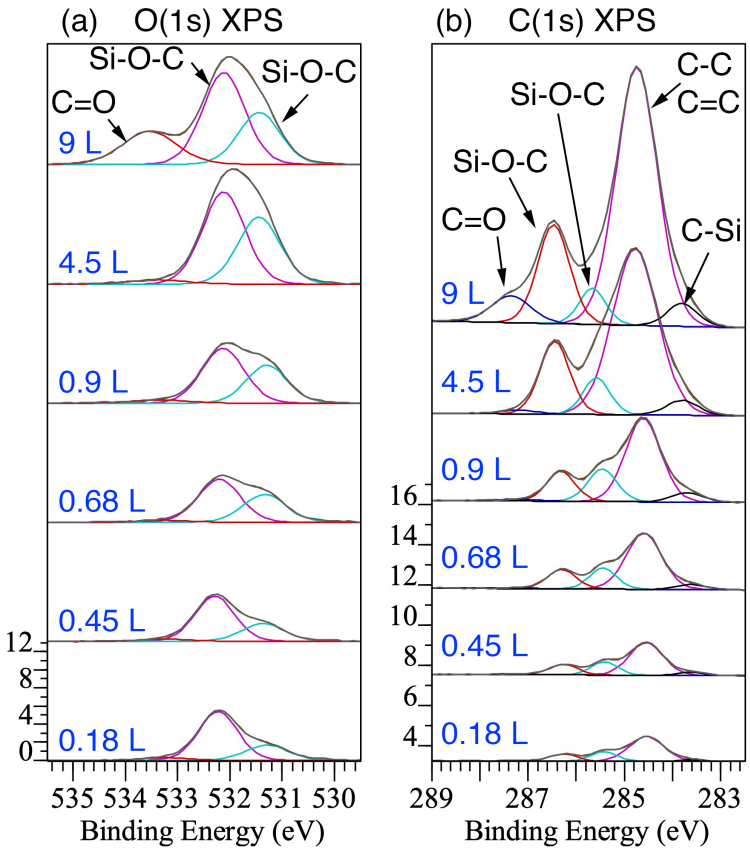

Figure 1: X-ray photoelectron spectroscopy (XPS) measurements of p-methoxyacetophenone exposed Si(001) surfaces as a function of p-methoxyacetophenone dose from 0.18 L to 9 L. (a) O(1s) spectra with peaks at 531.4 (strained Si-O-C), 532.1 (Si-O-C), and 533.5 eV (C=O). There is also a small contamination peak at 532.8 eV that does not vary with dose; this peak can be attributed to the adsorption of H_2O from the background during sample preparation. (b) C(1s) spectra with peaks at 283.8 (C-Si), 284.7 (C-C/C=C), 285.7 (C-O-Si), 286.5 (C-O-Si), and 287.4 eV (C=O). The quoted energies are for the 9 L dose; there is a systematic band bending shift to lower binding energy for the lower doses with a maximum shift of 0.2 eV for the 0.18 L dose.

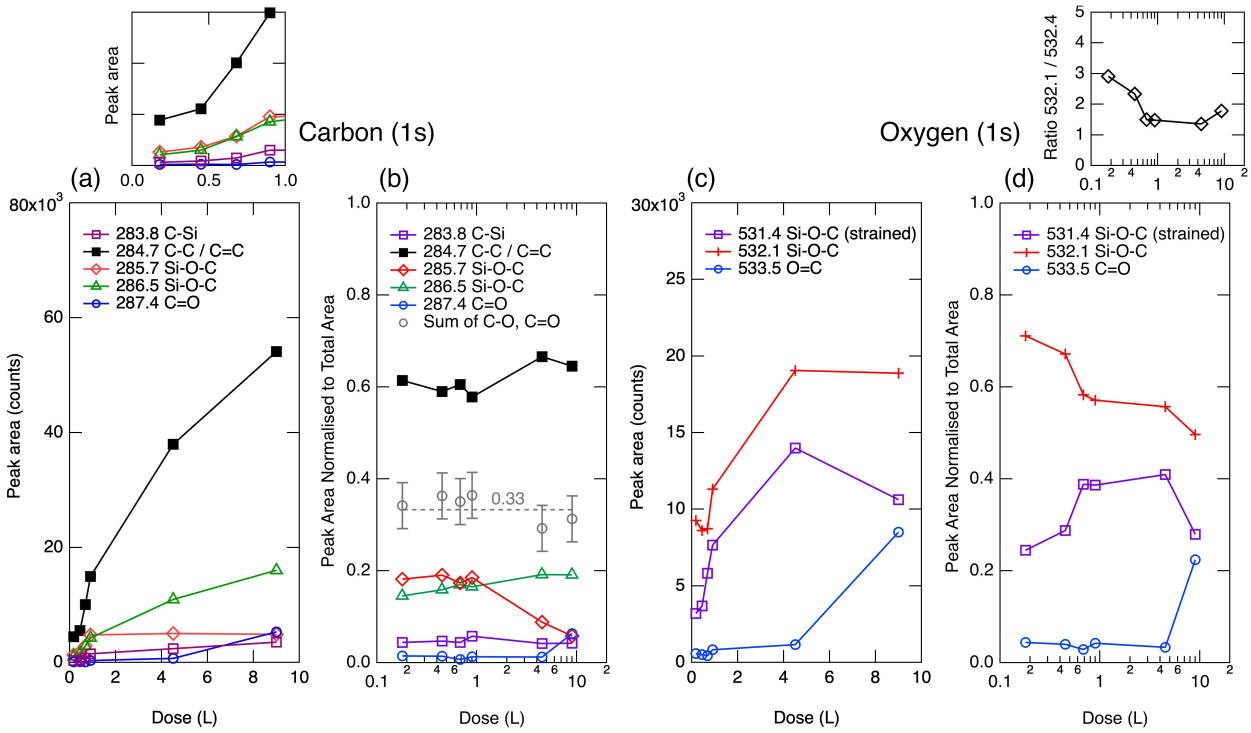

Figure 2: Variation of oxygen (1s) and carbon (1s) XPS peak areas as a function of methoxyacetophenone dose. (a) C(1s) peak areas. The inset shows an enlargement of the initial dose region up to 1 L. (b) Same data as panel (a) but plotted as relative peak areas (total area for all peaks = 1) on linear-log plot. Gray open circles show the addition of 285.7, 286.5 and 287.4 eV peaks and the dashed line indicates 33.3% coverage. (c) O(1s) peak areas as a function of dose. (d) Relative peak areas for each of the three O(1s) peak components. The inset shows the ratio of the 532.1 and 531.4 eV peaks.

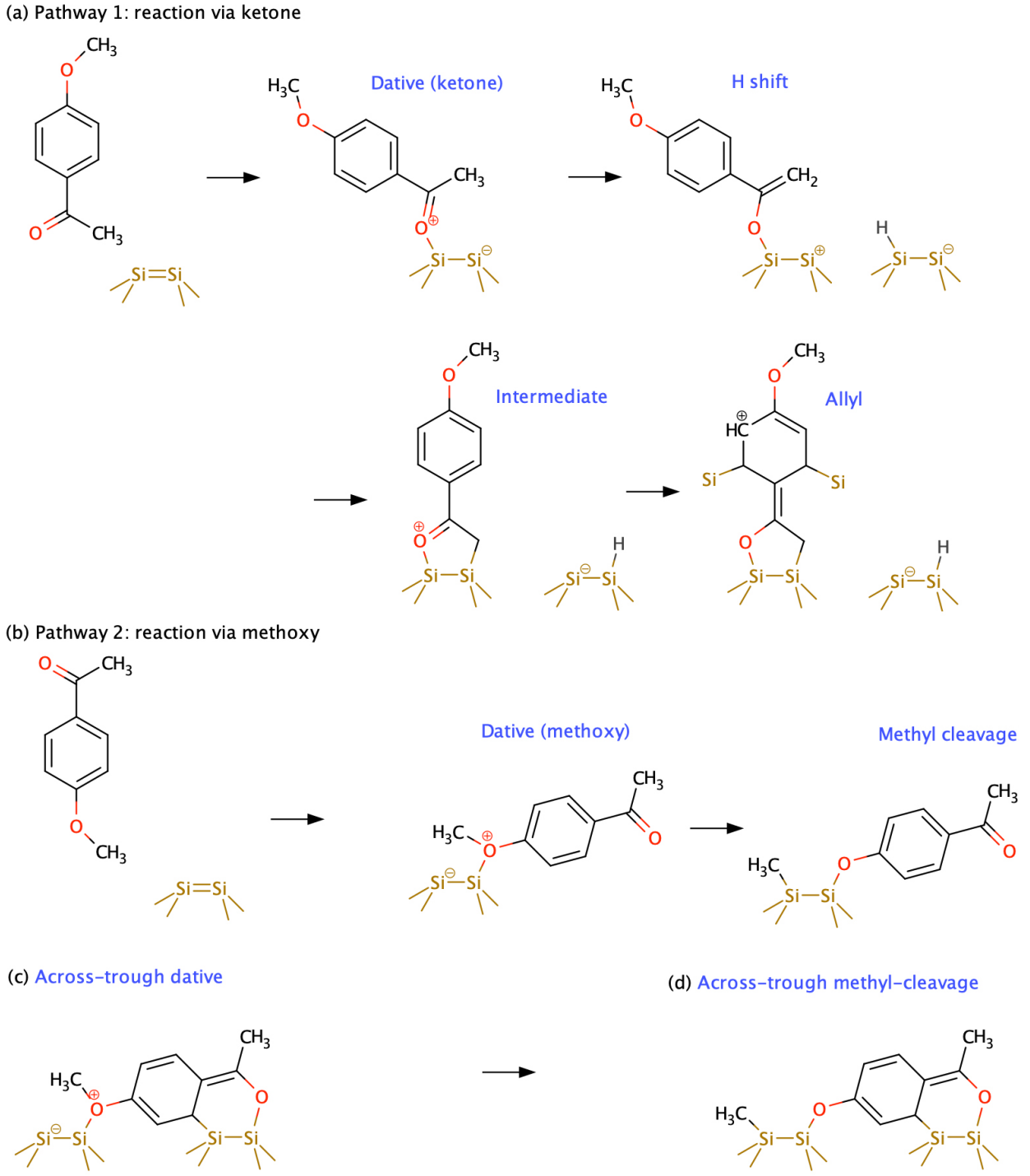

Figure 3: Anticipated reaction pathways for methoxyacetophenone on Si(001). (a) Pathway 1: methoxyacetophenone forms a dative bond to the surface via the ketone oxygen, followed by a proton shift and the formation of three Si-C bonds as indicated. This pathway can be expected to occur by analogy with the reaction of acetophenone on Si(001).[6,7] (Note that the two apparently isolated Si atoms in the allyl structure are in fact part of the same Si–Si dimer; full coordinates for all structures are available online at https://doi.org/10.5281/zenodo.2650188). (b) Pathway 2: reaction via the methoxy leads to a dative bound structure that can stabilise via methyl cleavage. (c) The combination of Pathways 1 and 2 can result in adsorbates attached via the oxygen atoms at each end of the molecule across a silicon dimer trough.

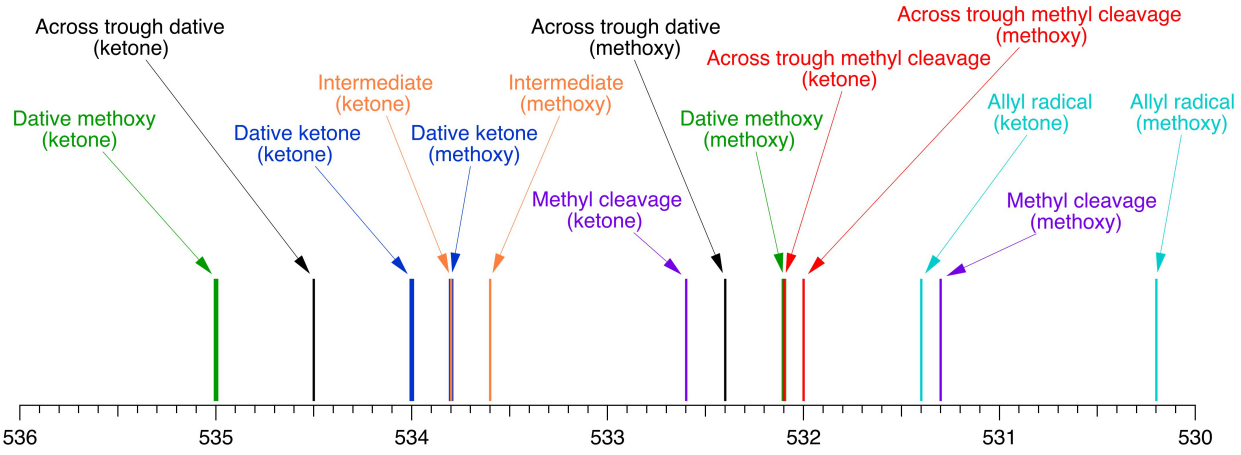

Figure 4: Calculated O(1s) binding energies in electronvolts. The structure names correspond to those shown in Fig. 3. Each structure produces a pair of peaks from the methoxy and ketone oxygen atoms, respectively. Binding energy values can be read from the axis and are also tabulated in Supplementary Table S1. These O(1s) binding energies were predicted based on Koopmanns theorem similarly to the approaches previously reported by the Teplyakov group for N(1s) features[47,48] and calibrated against experimental data for molecular acetone (532.7 eV multilayer acetone;[17]) and methanol[18] to produce expected difference between computationally predicted and experimental values of +11.4 eV. The exact values predicted by this approach have been shown to be very consistent with the experimental data, although the predicted differences in energy among the computed structures are expected to be more reliable than the exact binding energies.

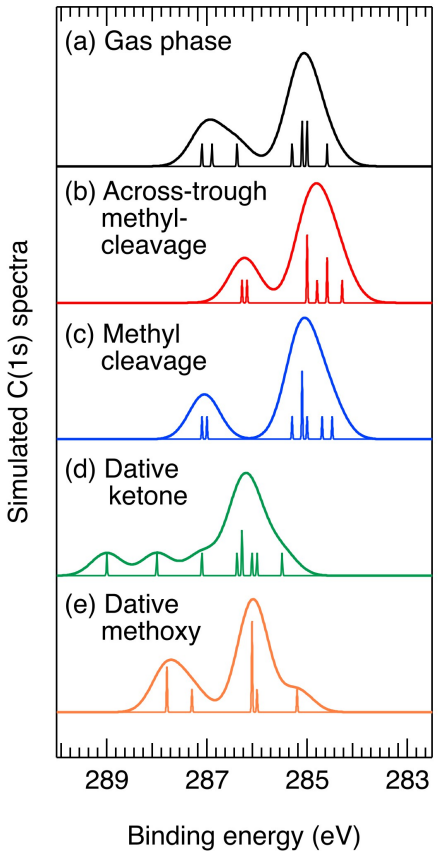

Figure 5: Simulated C(1s) XPS spectra: (a) gas phase methoxyacetophenone, (b) trough-bridge methyl cleavage, (c) methyl cleavage, (d) dative ketone, and (e) dative methoxy. The calculated binding energies are tabulated in Supplementary Table S2. The narrow peaks represent the location of individual binding energy components; when more than one carbon produces the same binding energy (the calculated energy resolution was 0.1 eV) the height of the narrow peak is increased. The individual components have been convoluted with a Gaussian (FWHM 0.9 eV) to produce a spectrum that can be compared to the experimentally measured spectra.

Table 1: X-ray photoelectron spectroscopy (XPS) peak energies for various organic compounds adsorbed to Si(001) taken from the references indicated. Methyl iodide adsorbs dissociatively such that this data represents Si-CH_3 species. PQ and CHD represent 9,10-phenanthrenequinone and 1,2-cyclohexanedione, respectively.[31] The "Si-C (strong)" column represents either strong Si-C bonding, as occurs for Si-CH_3, or the formation of silicon-carbide alloys, e.g., that form as a result of annealing a silicon surface after organic deposition. The "Si-C-R" represents Si-C bonding where a molecular fragment is attached to silicon resulting in a somewhat weaker Si-C bond.

Adsorbate	Carbon (1s)					Oxygen (1s)		
Assignment	Si-C (strong)	Si-C-R	C-C / C=C	Si-O-C	C=O	Si-O-C	C=O	Reference
Methyl iodide	283.2♮	284.1						30
Ethylene		284.0						20
Ethylene	282.8♮	284.0, 283.3*						21
Ethylene		283.95, 283.38*						22
Acetylene		284.1	284.9					20
Acetylene		283.7, 284.07*						22
Cyclopentene		284.1	284.9					20
Cyclopentene		284.3	284.8‡					27
3-pyrroline		284.1	284.8, 285.7					20
Benzene		283.9	284.2					28
C_{60}		283.8	284.5, 285.3†					29
Methanol				286.6		532.2		33
Methanol			284.4	286.6		532.3		31
Phenol			285.1	286.6		532.5		32
Acetaldehyde	282.6	284.5	285.2♭ , 285.4		287.7♭	532.4, 531.5‡	532.7♭	17
Acetone	282.6	284.5	285.2♭, 285.5		287.6♭	532.5, 531.4‡	532.7♭	17
Acetophenone	283.4	284.2	284.5	286.3, 285.9				6
PQ			284.6	286		532.5		31
CHD			285	285.8		532.4		31

♮ After annealing.

* Possibly vibrationally shifted from the main Si-C peak.

† Electrostatically shifted 0.8 eV in the monolayer.

‡ These lower energy peaks we attribute to the strained four membered ring C-O-Si-Si di-σ configuration.[34,36]

♭ These peaks obtained from multilayers formed at low temperatures.[17]

Table 2: XPS peak assignments with references to similar values in the literature

Region	Peak energy (eV)	Peak Assignment	Reference
3*O(1s)	531.4	Si-O-C (strained)	[17,34,36]
	532.1	Si-O-C	[17,34,36]
	533.5	C=O	[17]
5*C(1s)	283.8	C-Si	[20]
	284.7	C-C / C=C	[20]
	285.7	Si-O-C #1	[32]
	286.5	Si-O-C #2	[32]
	287.4	C=O	[17]

Table 3: Calculated adsorption energies for select structures shown in Fig. 3. Structures were optimised using the LANL2DZ functional and a single-point energy calculation was performed using 6-311++G(d,p).

2*Structure	Energy (eV) LANL2DZ	Energy (eV) 6-311++G(d,p)
Dative (methoxy)	-0.42	-0.77
Dative (ketone)	-1.00	-1.32
Across-trough dative	-1.81	-2.36
Intermediate	-2.26	-2.54
Methyl cleavage	-3.32	-3.63
Across-trough methyl cleavage	-4.58	-5.18

Graphical TOC Entry